Title

A Framework for Probabilistic Assessment of Liquefaction Manifestation

Authors

Hudson, Kenneth S
Ulmer, Kristin
Brandenberg, Scott J
et al.

Publication Date

2024-02-22

DOI

10.1061/9780784485316.017

Peer reviewed

A Framework for Probabilistic Assessment of Liquefaction Manifestation

Kenneth S. Hudson, P.G.[1]; Kristin Ulmer, Ph.D.[2]; Scott J. Brandenberg, Ph.D., P.E.[3]; Paolo Zimmaro, Ph.D.[4]; Steven L. Kramer, Ph.D.[5]; and Jonathan P. Stewart, Ph.D., P.E.[6]

[1]Dept. of Civil and Environmental Engineering, UCLA. Email: kenneth.s.hudson@gmail.com
[2]Southwest Research Institute. Email: kulmer@swri.org
[3]Dept. of Civil and Environmental Engineering, UCLA. Email: sjbrandenberg@g.ucla.edu
[4]Department of Environmental Engineering, Univ. of Calabria, Italy.
Email: paolo.zimmaro@unical.it
[5]Dept. of Civil and Environmental Engineering, Univ. of Washington. Email: kramer@uw.edu
[6]Dept. of Civil and Environmental Engineering, UCLA. Email: jstewart@seas.ucla.edu

ABSTRACT

As part of the next generation liquefaction (NGL) project, we are developing probabilistic triggering and manifestation models using laboratory data and cone penetration test (CPT) case histories in the NGL database. The case histories are used to develop probabilistic models for surface manifestation conditional on susceptibility, liquefaction triggering, soil properties, stratigraphic details, and other features. Susceptibility is interpreted as a sole function of soil composition and is expressed as a probabilistic function of soil behavior type index, I_c, obtained from CPT. A triggering model is derived based on laboratory tests on high-quality specimens from literature; this model captures mean responses and uncertainty reflective of data dispersion and is considered as a Bayesian prior that will subsequently be updated by field observation data. A manifestation model is then regressed from field case histories where surface manifestation was or was not observed, information on soil conditions that enables identification of layers likely to liquefy, and ground shaking conditions. We describe the approach applied to develop our manifestation model; for a given layer this model considers layer depth, thickness, CPT tip resistance, and I_c. The result of this process is a logistic function in which manifestation probability decreases with increasing depth, decreasing thickness, increasing tip resistance, and increasing I_c. Profile manifestation is then derived by aggregating individual layer manifestation probabilities.

INTRODUCTION

A three-step process is typically used to judge seismic hazards related to soil liquefaction, namely: (1) evaluation of liquefaction susceptibility, (2) evaluation of the potential for loss of stiffness and strength from liquefaction triggering, and (3) assessment of likely consequences of liquefaction or cyclic softening (e.g., instabilities or deformations). Case histories of field performance from liquefaction necessarily contain information on soil conditions and ground shaking (e.g., Stewart et al. 2016), but the condition that mainly limits their numbers is the requirement for post-earthquake observations of manifestation or lack thereof in past earthquake events. As a result, the case histories most directly provide information on the manifestation consequence, whereas in past work manifestation has generally been interpreted as being uniquely associated with triggering and lack of manifestation with no-triggering (e.g., Cetin et al. 2004 and 2018; Idriss and Boulanger, 2008; and Boulanger and Idriss 2012 and 2016).

We take a different approach in which observation of surface manifestation or lack thereof is taken as only providing evidence of field performance and not (directly) whether liquefaction was or was not triggered. Using case histories in the Next Generation Liquefaction (NGL) Project database (Ulmer et al. 2023a, Brandenberg et al. 2020), we are developing a model for liquefaction manifestation of a soil profile that considers the manifestation potential of individual layers. For each triggered layer, manifestation is related to layer depth, thickness, corrected CPT tip resistance (q_{c1N} or q_{c1Ncs}), and I_c. The triggering is derived from laboratory cyclic test results, which has been separately presented (Ulmer et al. 2023b, Carlton et al. 2022); the focus of this paper is on presenting the framework being used to develop the manifestation model. The model itself is under development, and results presented herein are merely for illustrative purposes.

SEPARATING TRIGGERING FROM MANIFESTATION

Surface manifestation of liquefaction generally takes the forms of sediment boils, ground cracks, or similar effects. Historically, it has been common to interpret manifestation at case history sites as equivalent to triggering and absence of manifestation as indicating that triggering did not occur. However, it is possible for sand boils to develop at sites where thick, shallow, susceptible layers produce significant pore pressures that do not exceed the level of initial liquefaction (i.e., pore pressure ratio r_u = 1.0) (Tokimatsu et al., 2012; Kramer et al., 2016). Furthermore, it is possible for liquefaction to be triggered in thin, deep susceptible layers without producing surface manifestation.

Examples. Figure 1 shows a CPT profile for Wufeng Site A (Chu et al. 2008) that did not manifest liquefaction during the 1999 Chi-Chi earthquake. There are three layers labeled 4, 6, and 8 that have I_c values near or less than 2.6 and are therefore interpreted as being sand-like and susceptible to liquefaction, and a low q_{c1Ncs}. Shaking intensity was strong for this site, and the magnitude- and overburden-corrected *CSR* (CSR_M) values at the depth of the layers is between 0.6 to 0.85 based on processing steps by Boulanger and Idriss (i.e., r_d, *MSF*, etc.). These layers are predicted to liquefy by all published liquefaction models, but the site did not exhibit manifestation. We postulate that liquefaction did trigger in some or all of these layers but did not manifest due to the presence of the thick clay-like crust layer that is not susceptible to liquefaction. Furthermore, this profile exhibits significant interbedding, which has been associated with lack of surface manifestation at many sites in Christchurch, New Zealand. Sandy layers within these profiles would also be predicted to liquefy based on current liquefaction models (Cubrinovski et al., 2019, Hutabarat and Bray, 2021, 2022), but as in Wufeng, the non-manifestations in these examples point to the importance of separating triggering from manifestation in analysis.

Probabilistic Framework. The historical use of manifestation as an indicator of liquefaction triggering and lack of manifestation as an indicator of a lack of triggering implies that the probability of triggering is equal to the probability of manifestation, i.e., $P[T] = P[M]$, and the probability of no triggering is equal to the probability of no manifestation $P[NT] = P[NM]$. We take a different approach by utilizing Bayes' theorem to interpret relationships between triggering and manifestation. Consider for example the probability that the soil in the critical layer triggered conditioned on manifestation having been observed, i.e., $P[T|M]$,

$$P[T|M_L] = \frac{(P[M_L|T]P[T])}{P[M]} = \frac{(P[M_L|T]P[T])}{(P[M_L|T]P[T] + P[M_L|NT]P[NT])} \quad (1)$$

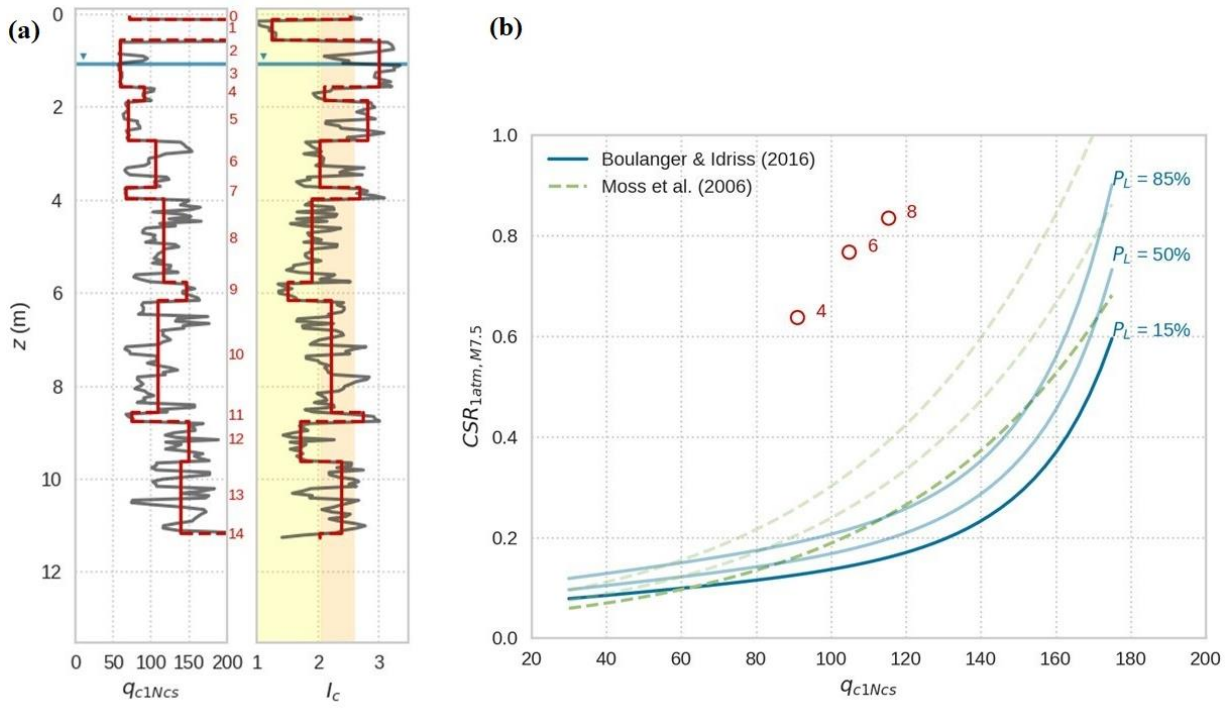

Figure 1. (a) CPT WAC-3 from Wufeng Site A in Taiwan (Chu et al. 2008), with no surface manifestation of liquefaction despite having loose, sand in Layers 4, 6, and 8. (b) Critical layer values of q_{c1Ncs} and *CSR* plotted on traditional triggering curves from Boulanger and Idriss (2016) and Moss et al. (2006).

Table 1 lists three probabilities – those of triggering $P[T]$, manifestation of a layer given triggering $P[M_L|T]$, and manifestation of a layer given no triggering $P[M_L|NT]$, where the subscript "L" denotes the manifestation from a single layer. Other pertinent probabilities can be computed from their complements, e.g., $P[NT] = 1 - P[T]$.

Table 1. Descriptions of Probabilities in our Approach

Term	Definition
$P[S]$	Probability of susceptibility (e.g., Mauer et al. 2017)
$P[T]$	Probability that a layer triggers. Note that $P[T] = P[S]*P[T\|S]$
$P[M_L\|T]$	Probability that a layer causes surface manifestation given that it triggers.
$P[M_L\|NT]$	Probability that a layer causes surface manifestation given that it does not trigger. This may result from high pore pressures (but not high enough to trigger liquefaction) that cause sand boils or other observations we usually interpret as manifestation of liquefaction.

Probability of Triggering. We utilized laboratory test data to develop a prior distribution for $P[T]$ conditioned on relative density and *CS*R (Ulmer et al. 2023b, Carlton et al. 2022). This work is presented in Ulmer et al (2023c) and is omitted here due to length limitations. The laboratory-based prior will subsequently be investigated for potential revision using Bayesian inference.

MODEL FRAMEWORK FOR PROFILE MANIFESTATION

The framework computes a probability of profile manifestation based on probabilities of manifestation of each soil layer within the profile, which in turn is conditioned on the probabilities that each layer within the profile will trigger, along with other layer features. This framework does not require identification of a critical layer within the profile; rather we aggregate contributions of each layer (denoted with the subscript "*L*") to the profile manifestation probability to compute the profile manifestation probability, $P[M_P]$, where the subscript "*P*" denotes profile. Layer boundaries and representative values can be interpreted from CPT profiles using judgement or algorithms (e.g., Hudson et al. 2023). Terminology is defined in Table 2.

Table 2. Terminology for profile manifestation model

Term	Definition
N_L	Number of layers in profile
i	Layer index counter
β	Model coefficient
$P[M_L]$	Probability that layer causes surface manifestation

Layer Manifestation Probability. The probability that a layer will manifest is computed using a logistic function. For example, Eq. 2 is a multivariate logistic function expressing probability of manifestation as a function of q_{c1N}, I_c, and depth to the top of the layer (z_{top}).

$$P\left[M_L|T\right] = \frac{1}{1 + e^{-(\beta_0+\beta_1 \cdot q_{c1N}+\beta_2 \cdot I_c+\beta_3 \cdot z_{top})}} \tag{2}$$

where β_0 to β_3 are regressed coefficients.

Figure 2 plots the resulting logistic function. The probability factor depends jointly on all three features, so multiple plots are required to demonstrate key aspects of the function. As evidenced in the top left subplot of Figure 2, a layer at the ground surface (z_{top} = 0m) with I_c = 1 (represented as the darkest blue curve) has $P[M_L|T] \sim 1$ at $q_{c1N} < 75$. As q_{c1N} increases, $P[M_L|T]$ decreases until it is approximately 0 at q_{c1N} = 300. As I_c increases (the color of the curve gets warmer), for the same z_{top} and q_{c1N}, the $P[M_L|T]$ decreases. Moving to different subplots from left to right and top to bottom, as z_{top} increases $P[M_L|T]$ decreases for the same q_{c1N} and I_c values. We are currently exploring many different layer features, and the functions in Figure 2 are presented as preliminary results to illustrate the methodology.

Manifestation Probability of a Profile. The probability of manifestation of a profile $P[M_P]$ is computed using Eq. 3, where N_L is the number of layers in the profile, t_i is the thickness of the i^{th} layer, and t_c is a constant characteristic thickness. Eq. 3 consists of multiple components that

warrant separate discussions. First, the expression 1 - P[M_L|T]P[T] is equal to the probability that the layer will not manifest liquefaction, P[NM_L] = 1 - P[M_L]. If none of the layers manifest liquefaction, then the profile does not manifest liquefaction. Therefore, P[NM_P] is computed as a product sum of P[NM_L]. However, a direct product sum (i.e., without the t/t_c term in the exponent) inherently assumes that P[NM_L] for each layer is statistically independent from all other layers. This is generally not true. For example, consider a profile composed of a 3m thick layer with P[M_L|T] = 0.2 and P[T_L] = 1.0. In this case, Eq. 3 would produce P[M_P] = 0.2, which is the same as P[M_L|T] since the layer and the profile are one and the same. However, if we sub-divide the profile into three 1m thick layers each with P[M_L|T] = 0.2 and P[T] = 1.0, and we compute a product sum without the t_i/t_c exponent, then Eq. 3 produces P[M_P] = 0.488. This is an undesired outcome because the profile is the same in both cases, but the computed P[M_P] depends strongly on discretization of the profile.

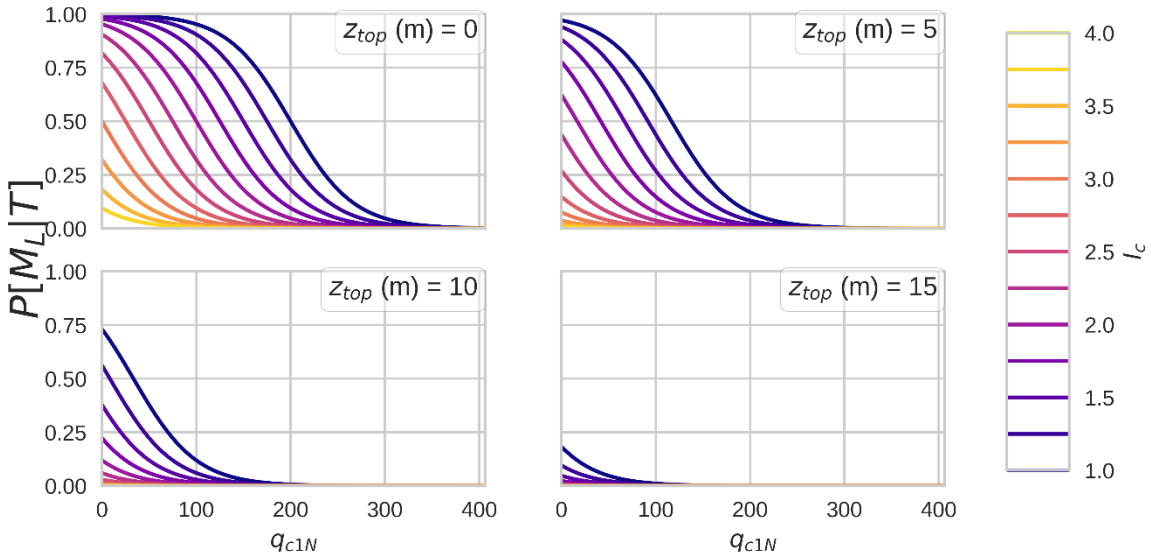

Figure 2. Logistic function illustrating effects of overburden corrected cone tip resistance, q_{c1N}, and soil behavior type index, I_c for reference top of the layer depths, z_{top}.

To overcome this discretization problem, we introduce the t_i/t_c exponent. If the same 3m thick layer has P[M_L|T] = 0.2, P[T] = 1.0, and t_c = 3m, then Eq. 3 provides P[M_P] = 0.2. If the layer is subdivided into three 1m thick layers, then Eq. 3 provides P[M_P] = 0.2. The t_i/t_c exponent has removed the influence of discretization by tying layer thickness to the characteristic length. The characteristic thickness is the layer thickness for which P[M_L|T] is statistically independent of the other layers. If all layers have a thickness equal to the characteristic thickness, then Eq. 3 reduces to a simple product sum. If a layer is thicker than the characteristic thickness, it becomes more likely to manifest, and vice versa, as illustrated in Figure 3. We considered including thickness as a variable within the logistic regression instead of as an exponent, but ultimately decided to include it as an exponent instead for this reason.

$$P\left[M_P\right] = 1 - \prod_{i=1}^{N_L} \left(1 - P\left[M_L|T\right]_i \cdot P[T]_i\right)^{t_i/t_c} \tag{3}$$

Consider the example profile in Figure 4, which has three layers with thicknesses of 3 m (also using t_c = 3m for simplicity), and groundwater table at the ground surface. Layer 1 has a high q_{c1N} and I_c (300 and 3.2, respectively), layer 2 has a low q_{c1N} and high I_c (50 and 3.2, respectively), and layer 3 has low q_{c1N} and low I_c (50 and 1.5, respectively). A strong motion with CSR=0.6 is assumed. The first step is to compute P[T|S] for each layer; layer 1 has P[T|S]~0 due to its high q_{c1N}, whereas layers 2 and 3 have relatively low q_{c1N} and high CSR, therefore P[T|S]~1. The P[S] is low for layers 1 and 2 due to high I_c. The product of P[T|S] and P[S] is P[T], which is 0, 0, and 1 for layers 1, 2, and 3 respectively. The logistic functions in Figure 2 and Eq. 2 are used with the profile data to compute P[M_L|T]. Layer 1 has P[M_L|T]=0, layer 2 has P[M_L|T]=0, and layer 3 has P[M_L|T]=0.5. These results are combined in Eq. 3 to provide profile manifestation probability P[M_P]=0.5, which is entirely caused by layer 3.

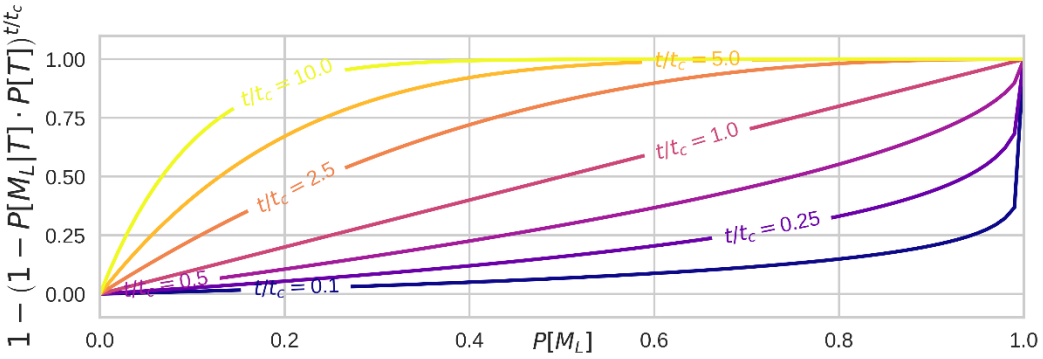

Figure 3. Influence of t/t_c exponent on probability of layer manifestation.

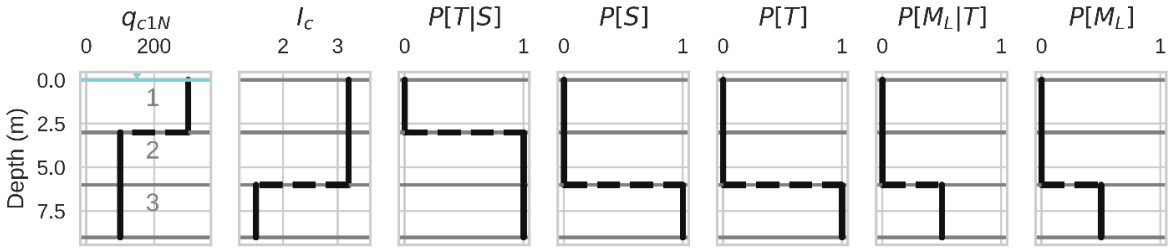

Figure 4. Simplified CPT profile demonstrating the computation of P[M^P].

PROFILE-BASED REGRESSION FRAMEWORK

The profile-based framework provides a value of $P[M_P]$ for a profile conditional on the properties of the layers within the profile, $P[T|S]$ and $P[S]$ for each layer, and the coefficients within the logistic functions. Independently regressing the logistic coefficients, $P[T|S]$ and $P[S]$ based on case history data was not attempted because (i) the amount of field case history data is inadequate to isolate so many different components, and (ii) there is a body of knowledge from laboratory testing that help us constrain $P[S]$ and $P[T|S]$. Our approach is therefore to develop prior distribution functions for $P[S]$ and $P[T|S]$, and subsequently use Bayesian inference to obtain posterior distributions following regression of the logistic coefficients. This section

develops a regression framework that solves for the logistic function coefficients based on observations of manifestations at NGL sites. We assume $P[M_L|NT]=0$ for this derivation, but we anticipate including it in future versions of the model.

Frequentist regression requires a cost function J that must be minimized, while Bayesian inference requires a likelihood function L that must be maximized. In least-squares regression, constants are selected to minimize the sum of the square of the difference between the predictions and observations. This form of regression is not well-suited to binary observations, such as whether liquefaction did or did not manifest at a site, because the dependent variable is not continuous. Logistic regression is better suited to this purpose. We herein seek values of the logistic coefficients that minimize the cost function J given by Eq. 4, where y_k is a binary indicator of whether manifestation was observed at the k^{th} site (y_k = 1 if manifestation was observed, y_k=0 if it was not), and N_P is the number of profiles.

$$J = -\frac{1}{N_P}\sum_{k=1}^{N_P}\left[y_k \ln\left(P\left[M_P\right]_k\right) + \left(1-y_k\right)\ln\left(1-P\left[M_P\right]_k\right)\right] \tag{4}$$

The cost function exhibits several notable properties. First, if y_k=1, only the first expression contributes to the cost function for profile k, whereas if y_k=0, only the second expression contributes. Second, if the prediction is a true positive (i.e., if y_k=1 and $P[M_P]_k$ = 1), or a true negative (i.e., if y_k=0 and $P[M_P]_k$ = 0), the contribution to the cost function from that profile is zero. Only values of $P[M_P]$ that do not match the observed manifestation contribute to the cost function. The ideal scenario would therefore be to select an optimal set of β's that render $P[M_P]$ values that are either 0 or 1 and match the observations. In that case, the cost function would be J = 0. For real datasets, this is generally not feasible, and the value of J will therefore be larger than zero. To perform the minimization, the cost function must be written in terms of the desired regression variables, which is obtained by substituting Eq. 2 and 3 into Eq. 4.

Traditional logistic regression problems are convex (i.e., they exhibit a single minimum) and are well-suited to convex optimization strategies like the gradient descent method. Unfortunately, the functional form we have adopted, which is a product of many multi-variate logistic functions raised to a power, is not convex. As a result, we must constrain the values of the model coefficients within a range of interest and try multiple initial guesses of the model coefficients to identify the minimum value of the cost function within the permissible space. We have adopted the limited memory Broyden–Fletcher–Goldfarb–Shanno constrained algorithm (Byrd et al., 1995), often called *L-BFGS-B* to solve this problem.

CONCLUSIONS AND NEXT STEPS

We have provided here a preliminary framework for separating the effects of liquefaction susceptibility, triggering, and manifestation during model development. These models represent "works in progress" and are not final recommendations. However, our framework presents useful steps towards more robust, fully probabilistic and performance-based approaches to assessing liquefaction potential. In this manuscript, we clarified the meaning of key terms in liquefaction analysis and provided a framework by which the different effects can be evaluated in a consistent and rational manner that is probabilistic and performance-based. We are continuing to explore other options in the model formulation including "profile-based" variables (e.g., interbeddedness of a profile, H_1, and liquefaction potential index), alternative demand parameters (*PGV*, *CAV*),

and contributions to manifestation from ground failure caused by cyclic softening of clay-like soils. Future work will expand this framework to consider SPT and boring log data as a stand-alone model or as a combined model with CPT.

ACKNOWLEDGEMENTS

"This work was supported with US Nuclear Regulatory Commission (Contract # 31310018D0002) and US Bureau of Reclamation (contract # R20PG00126) support via the Geosciences and Engineering Dept. of the Southwest Research Institute. This paper is an independent product and does not necessarily reflect the view or regulatory position of the NRC or the USBR. The authors wish to acknowledge members of the NGL Advisory Board and other NGL Modeling Teams for their helpful insights. The work presented here does not necessarily represent the opinions, concurrence, or desired approaches of other NGL teams.

REFERENCES

Boulanger, R. W., and I. M. Idriss. (2016). "CPT-Based Liquefaction Triggering Procedure." *Journal of Geotechnical and Geoenvironmental Engineering*, 142(2).

Boulanger, R. W., and I. M. Idriss. (2012). "Probabilistic Standard Penetration Test-based Liquefaction-Triggering Procedure." *Journal of Geotechnical and Geoenvironmental Engineering*. Vol. 138, No. 10. pp. 1,185–1,195.

Brandenberg, S. J., et al. (2020) "Next-Generation Liquefaction Database." *Earthquake Spectra*. Vol. 36, No. 2. pp. 939–959.

Byrd, R. H., P. Lu, J. Nocedal, and C. Zhu. (1995). "A Limited Memory Algorithm for Bound Constrained Optimization." *SIAM Journal on Scientific Computing*. Vol. 16, No. 5. pp. 1,190-1,208.

Carlton, B., K. Ulmer, T. Nguyen, and Q. Parker. (2022). *Next Generation Liquefaction (NGL) - Supporting Studies: Overburden and Initial Shear Stress*. DesignSafe-CI.

Cetin, K. O., R. B. Seed, A. Der Kiureghian, K. Tokimatsu, L. F. Harder, R. E. Kayen, and R. E. S. Moss. (2004). "Standard Penetration Test-Based Probabilistic and Deterministic Assessment of Seismic Soil Liquefaction Potential." *Journal of Geotechnical and Geoenvironmental Engineering*. Vol. 130, No. 12. pp. 1,314–1,340.

Cetin, K. O., R. B. Seed, R. E. Kayen, R. E. S. Moss, H. T. Bilge, M. Ilgac, and K. Chowdhury. (2018). "SPT-Based Probabilistic and Deterministic Assessment of Seismic Soil Liquefaction Triggering Hazard. *Soil Dynamics and Earthquake Engineering*. Vol. 115. pp. 698–709. (Accessed date 27 August 2022).

Chu, D. B., J. P. Stewart, R. W. Boulanger, and P.-S. Lin (2008). Cyclic softening of low plasticity clay and its effect on seismic foundation performance, *J. Geotech. & Geoenv. Engrg.*, 134 (11), 1595-1608.

Cubrinovski, M., A. Rhodes, N. Ntritsos, and S. van Ballegooy. (2019). "System Response of Liquefiable Deposits." *Soil Dynamics and Earthquake Engineering*. Vol. 124. pp. 212–229.

Hudson, K. S., K. J. Ulmer, P. Zimmaro, S. L. Kramer, J. P. Stewart, and S. J. Brandenberg (2023). Unsupervised Machine Learning for Detecting Soil Layer Boundaries from Cone Penetration Test Data, *Earthquake Engineering & Structural Dynamics*.

Hutabarat, D., and J. D. Bray. (2021). "Effective Stress Analysis of Liquefiable Sites to Estimate the Severity of Sediment Ejecta. *Journal of Geotechnical and Geoenvironmental Engineering*. Vol. 147, No. 5. (Accessed date 27 August 2022).

Hutabarat, D., and J. D. Bray. (2022). "Estimating the Severity of Liquefaction Ejecta Using the Cone Penetration Test. *Journal of Geotechnical and Geoenvironmental Engineering*. Vol. 148, No. 3. (Accessed date 30 August 2022).

Idriss, I. M., and R. W. Boulanger. (2008). *Soil Liquefaction During Earthquakes*. D. Becker, editor. Earthquake Engineering Research Institute.

Kramer, S. L., S. S. Sideras, and M. W. Greenfield. (2016). "The Timing of Liquefaction and Its Utility in Liquefaction Hazard Evaluation." *Soil Dynamics and Earthquake Engineering*. Vol. 91. pp. 133–146.

Maurer, B. W., S. van Ballegooy, L. M. Wotherspoon, and R. A. Green. (2017) "Assessing Liquefaction Susceptibility Using the CPT Soil Behavior Type Index." *3rd International Conference on Performance-based Design in Earthquake Geotechnical Engineering*. Vancouver.

Moss, R. E. S., R. B. Seed, R. E. Kayen, J. P. Stewart, A. Der Kiureghian, and K. O. Cetin. (2006). "CPT-based Probabilistic and Deterministic Assessment of In Situ Seismic Soil Liquefaction Potential." *Journal of Geotechnical and Geoenvironmental Engineering*. Vol. 132, No. 8. pp. 1,032–1,051.

Stewart, J. P., et al. (2016). PEER-NGL project: Open source global database and model development for the next-generation of liquefaction assessment procedures, *Soil Dyn. Earthquake Eng.*, **91**, 317–328.

Tokimatsu, K., S. Tamura, H. Suzuki, and K. Katsumata. (2012). "Building Damage Associated with Geotechnical Problems in the 2011 Tohoku Pacific Earthquake." *Soils and Foundations*. Vol. 52, No.5. pp. 956–74.

Ulmer, K. J., et al. (2023a). *Next-Generation Liquefaction Database, Version 2. Next-Generation Liquefaction Consortium*.

Ulmer, K. J., B. Carlton, T. Nguyen, and Q. Parker. (2023b). "An Expanded Data Set of Overburden (K_σ) and Initial Static Shear Stress (K_α) Correction Factors from Published Cyclic Laboratory Tests for Liquefaction Triggering Analyses." In *Geo-Congress 2023*, pp. 197-206.

Ulmer, K. J., K. Hudson, S. J. Brandenberg, P. Zimmaro, R. Pretell, B. Carlton, S. L. Kramer, and J. P. Stewart. (2023c) Task 7b: Draft Final Report Documenting Probabilistic Liquefaction Models. Report to USNRC and USBR. August 2023.